



## UvA-DARE (Digital Academic Repository)

### Abdominal aortic aneurysms

*The quest for meaningful biomarkers and opportunities to improve surgical care*

Jalalzadeh, H.

**Publication date**

2019

**Document Version**

Other version

**License**

Other

[Link to publication](#)

**Citation for published version (APA):**

Jalalzadeh, H. (2019). *Abdominal aortic aneurysms: The quest for meaningful biomarkers and opportunities to improve surgical care*. [Thesis, fully internal, Universiteit van Amsterdam].

**General rights**

It is not permitted to download or to forward/distribute the text or part of it without the consent of the author(s) and/or copyright holder(s), other than for strictly personal, individual use, unless the work is under an open content license (like Creative Commons).

**Disclaimer/Complaints regulations**

If you believe that digital publication of certain material infringes any of your rights or (privacy) interests, please let the Library know, stating your reasons. In case of a legitimate complaint, the Library will make the material inaccessible and/or remove it from the website. Please Ask the Library: <https://uba.uva.nl/en/contact>, or a letter to: Library of the University of Amsterdam, Secretariat, Singel 425, 1012 WP Amsterdam, The Netherlands. You will be contacted as soon as possible.

## CHAPTER 3

### T1 mapping of intraluminal thrombus of abdominal aortic aneurysms

#### *Preliminary results*

H. Jalalzadeh, R. Indrakusuma, P. de Heer, M.J. van der Laan, R.N. Planken,  
M.J.W. Koelemay, A.J. Nederveen, R. Balm

## ABSTRACT

### Introduction

T1 mapping is a magnetic resonance imaging (MRI) method that enables the quantification of tissue properties by calculation of tissue-specific T1 values. T1 mapping has not been carried out in intraluminal thrombus (ILT) of abdominal aortic aneurysm (AAA) before. If reproducible and accurate, T1 mapping could be used to monitor the natural course of ILT and its relation with AAA progression and rupture. This study determined the technical feasibility and reproducibility of T1 mapping of ILT of AAA. It also assessed whether T1 times, and the variability of T1 times within ILT are associated with AAA diameter or ILT thickness.

### Methods

This study was part of a larger prospective study titled 'Advanced MRI in AAA' study. Patients with AAA were included from Flevoziekenhuis hospital and Amsterdam UMC hospital, University of Amsterdam. Patients underwent MRI at 3.0 T twice on two separate days. This study reports the results of the first ten patients. After T1 map reconstruction and manual segmentation, the ILTs were divided into 6 segments and into an inner and outer layer. Reproducibility was tested by means of an intra-observer, inter-observer and inter-scan agreement analysis with calculation of intraclass correlation coefficients (ICCs) and coefficients of variation (CVs). Correlations were tested between AAA diameter and global mean T1 and the standard deviation (SD) of global mean T1 using Spearman's rho ( $\rho$ ). The correlation between ILT thickness and segmental mean T1 and the SD of segmental mean T1 was tested using the same method.

### Results

Eight patients were male and the median age was 71 y. The median AAA diameter was 47 mm. Global mean T1 was  $1381.1 \pm 449.9$  ms. Excellent intra-observer, inter-observer and inter-scan agreement was found for mean and median T1 values of the 10 global ILTs (ICC  $\geq 0.98$ , 95% CI 0.80 - 1.00). Intra-observer, inter-observer and inter-scan CV of segmental mean T1 was 5.47%, 7.42%, and 7.67%, respectively. A statistically significant low correlation was found between ILT thickness and SD of segmental mean T1 ( $\rho = 0.47$ ,  $p = 0.001$ ), suggesting that thicker ILT segments are more heterogeneous in composition. No correlation was found between AAA diameter and global T1 values. The inner ILT layers had higher T1 values than the outer layers in all but one AAA but this difference was not statistically significant ( $p = 0.22$ ).

**Conclusions**

T1 mapping of ILT in AAA is technically feasible and results are reproducible. Differences were observed between inner and outer ILT segments, and thicker ILT segments appear to be more heterogeneous in composition. T1 mapping can be a valuable tool to monitor ILT progression and to provide more information about the natural history of ILT and AAA.

## INTRODUCTION

The pathophysiology and natural course of abdominal aortic aneurysm (AAA) are insufficiently understood, despite the common prevalence of AAA and the large body of research regarding this disorder.<sup>1</sup> One of the key characteristics of many AAAs is the presence of intraluminal thrombus (ILT). ILT mainly consists of aggregated platelets and red blood cells which are held together by a mesh of fibrin proteins.<sup>2</sup> Studies have shown layered aspects within ILT, possibly representing different stages of growth and ageing, as well as a system of reticular channels (canaliculi) inside the ILT.<sup>2,3</sup> Because some histopathological studies have shown various proteases such as matrix metalloproteinase 9 within ILT, it has been suggested that ILT might be a dynamic and biologically active structure, rather than an inert substance.<sup>3,4</sup>

The role of ILT in AAA progression is not well known. Histopathological studies have shown associations between ILT presence and AAA progression. They have demonstrated that aneurysm wall segments covered by ILT are thinner and more hypoxic.<sup>5,6</sup> This could cause wall weakening and an increased risk of rupture.<sup>5</sup> This is confirmed by other studies showing signs of inflammation and neovascularization in aneurysm wall segments covered by ILT.<sup>6</sup> In contrast, biomechanical studies have attributed a protective effect of ILT against rupture. It is believed that ILT serves as a protective buffer which redistributes the biomechanical stress on the aortic wall.<sup>7,8</sup> However, recent studies have suggested that the protective biomechanical advantage of ILT might be outweighed by the weakening of the AAA wall.<sup>9</sup>

Studying ILT and its natural course is challenging. Histopathological examination of ILT is difficult because of its soft structure. In addition, ILT specimens generally are obtained at AAA repair and therefore provide information about the structure at a late development stage. Changes in ILT composition in the course of time are therefore unknown. Quantitative magnetic resonance imaging (MRI) techniques such as T1 and T2 mapping offer the possibility to quantify tissue-specific ILT characteristics at an early stage *in vivo*. T1 mapping has previously been used successfully for characterization of carotid plaques and to distinguish normal and abnormal myocardial tissues.<sup>10,11</sup> By creating a series of images with multiple inversion times, T1 relaxation times can be calculated for individual voxels, which directly correspond to variations in intrinsic tissue properties.<sup>10</sup> Unlike T1-, T2-, or T2\*-weighted images, this method of mapping not only allows visualization, but also quantification of structural properties.<sup>12</sup>

T1 mapping has not been carried out in ILT of AAA before. If reproducible and accurate, it could be used in future longitudinal studies to monitor the natural course of ILT and its relation with AAA progression and rupture.

The main objectives of this study were to assess the technical feasibility and reproducibility of T1 mapping of ILT of AAA. Other objectives were to assess whether T1 times, and the variability of T1 times within ILT are associated with AAA diameter or ILT thickness.

## METHODS

### Study design

This single-center prospective cross-sectional pilot cohort study was carried out in accordance with the Declaration of Helsinki.<sup>13</sup> The medical ethics board of Amsterdam UMC, University of Amsterdam, approved this study (2016\_121) prior to initiation. This manuscript was written in accordance with the STROBE statement.<sup>14</sup>

### Setting and study size

This study was part of a larger prospective MRI study titled 'Advanced MRI in AAA' (clinicaltrials.gov identifier NCT03138434). Patients were recruited from the outpatient clinic of the vascular surgery department of Amsterdam UMC hospital, University of Amsterdam, and of Flevoziekenhuis hospital in Almere from October 2017 to July 2018. The study phase was preceded by an optimization phase in which five patients were scanned once for optimization of the MR sequences. In the main study phase, 10 patients underwent MR imaging twice on two separate days with a time interval of  $7 \pm 5$  days between both scans.

### Participants

Patients were eligible for inclusion in the 'Advanced MRI in AAA' when they were 18 years or older and had an intact AAA with a diameter of at least 30 mm. Patients were excluded when they had contra-indications for MRI, a severely reduced renal function (eGFR < 30), previous allergic reaction to intravenous contrast agents, a suprarenal, pararenal, inflammatory, mycotic or infectious AAA, previous aneurysm repair, vasculitis or a connective tissue disease. For the current T1 mapping study, patients were excluded when no ILT was present or when the ILT was too thin for segmentation (i.e. <3 mm).

### Data acquisition

#### *MR acquisition*

All scans were performed on a 3.0 Tesla (T) Philips Ingenia MR scanner (Philips, Best, the Netherlands), according to a predefined protocol. The scanner was controlled by a team of two experienced MRI technicians and at least one researcher of the department of surgery. Image acquisition was performed on one slice that was positioned perpendicular

on the central aortic line. This slice was positioned between the maximal AAA diameter and the maximal ILT thickness. Screenshots of the slice position during the first scan were used for slice positioning on the second scan.

T1 mapping data was acquired using a vendor supplied breathhold T1 mapping sequence (MOLLI cardiac native) with a four-lead vectorcardiogram and a conventional torso coil. The imaging parameters were as follows: TE/TR 0.96/2.1 ms, field of view: 300x300 mm, slice thickness: 10 mm, voxel size: 2x2 mm, flip angle (FA): 20 degrees, reconstruction matrix 256x256. The scan time of the T1 mapping sequence was one breathhold of 11 s.

### *Segmentation*

Both the segmentation and the T1 map reconstruction were carried out with QMap (version 2.2.32, Medis, Leiden, the Netherlands). The segmentation of ILT was conducted manually on the raw images with a polygon tool with at least 15 dots. The drawn contours were transposed to the T1 map, the  $R^2$  map (explained below), the raw images of the different inversion times, additional post-contrast images, and adjusted when necessary. The ILT was afterwards divided into 6 segments (Figure 1). The mean T1 values and their corresponding standard deviations (SD) were automatically measured for both the global ILT area and for the ILT segments separately. The ILT was additionally segmented in an inner and outer layer to compare T1 values of the inner and outer layer of the ILT (Figure 1). The aortic lumen was separately segmented in an additional ROI to calculate the T1 values of the flowing blood in order to compare the results with previously published T1 values of circulating blood. AAA diameter and ILT thickness were measured manually with the same software on the same slice. AAA diameter was measured in the anteroposterior direction.

### *T1 map reconstruction*

The general method of T1 mapping involves the creation of a series of multiple images obtained at multiple inversion times (i.e. different time intervals between inversion of the longitudinal magnetization and measurement of the transversal magnetization) in order to determine the T1 relaxation times for different structures. Based on the series of images, a relaxation curve is estimated, and the T1 relaxation time is estimated. The T1 map was automatically reconstructed by the software, together with the  $R^2$  map of the coefficient of determination which demonstrates the goodness of fit of the model for individual pixels. All raw images were screened for the presence of motion artefacts prior to T1 map reconstruction. Artefacts were defined as black or white bands over the AAA. AAAs with artefacts were excluded from further analysis.

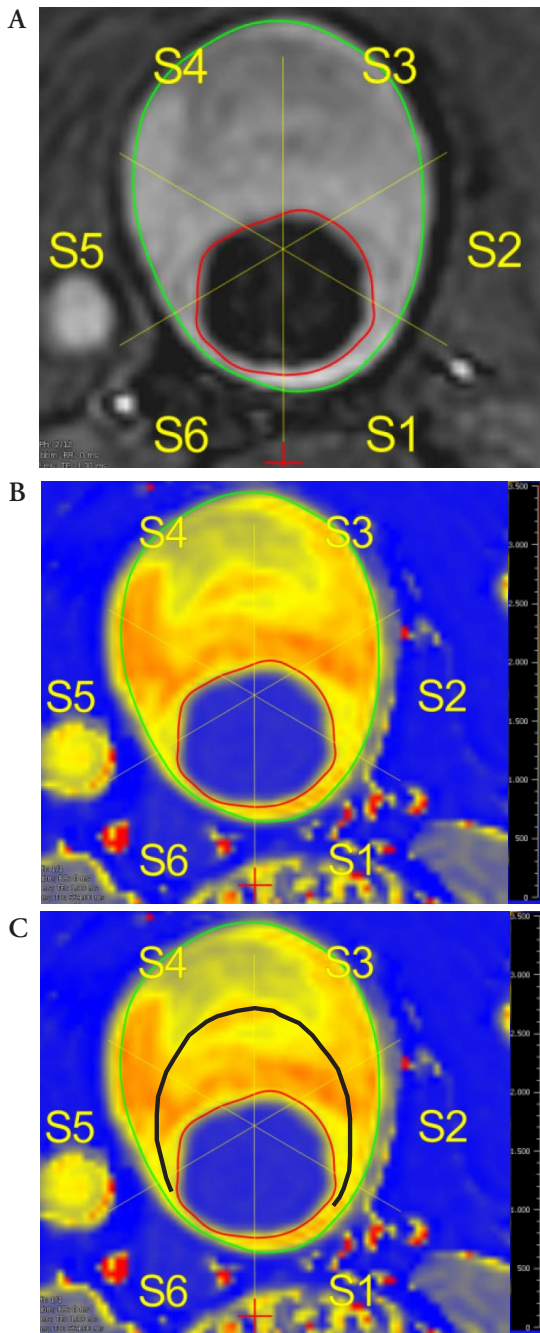


**Figure 1.** Example of one AAA with ILT divided in 6 segments: raw image (a), T1 map (b), T1 map with ILT divided in inner and outer layer (c).



## Parameters

The main outcome parameters were obtained from the T1 map of the global ILT and of the 6 segments separately (Figure 1). The obtained parameters for the global ILT were global mean T1, standard deviation (SD) of global mean T1, global median T1, global minimum (min) T1 and global maximum (max) T1. The parameters of the segments were segmental mean T1, SD of segmental mean T1, segmental median T1, segmental min T1, and segmental max T1. In order to compare the inner and outer ILT layers, an inner-to-outer ratio of mean T1 was calculated as:  $\text{mean T1}_{\text{inner layer}} / \text{mean T1}_{\text{outer layer}}$ .

The T1 variability within each ILT was additionally assessed by calculating the ‘mean absolute deviation of T1’ (madT1), which is the difference between each segmental mean T1 and the global mean T1. madT1 was calculated for all 6 ILT segments separately. This statistically-derived parameter previously has been used to assess T2 inhomogeneity in the myocardium, and quantifies within-subject variability without being affected by inter-subject variability.<sup>15,16</sup> Other variables included baseline patient characteristics and geometrical features such as AAA diameter and ILT thickness.

## Statistical methods

### *Reproducibility analysis*

Reproducibility was tested by means of an intra-observer, inter-observer and inter-scan agreement analysis. Agreement was tested for the mean T1 value of the total ILT and the mean T1 value of the 6 segments separately. A single observer (HJ) repeated the T1 map calculation and segmentation to test the intra-observer agreement. The same was done by two investigators (HJ, RI) to test the inter-observer agreement. After establishing good intra- and inter-observer agreement, a single observer (HJ) tested the inter-scan agreement in a similar fashion between the first and second scan of all patients.

Intra-observer, inter-observer, and inter-scan agreement was tested by calculating intraclass correlation coefficients (ICCs) with corresponding 95% confidence intervals (CI). ICC was calculated for the absolute agreement of single measures. This was done with a two-way random effects model for the inter-observer agreement, and with a two-way mixed effects model for the intra-observer and inter-scan agreement.<sup>17</sup> ICC values were considered as poor, moderate, good, and excellent agreement when <0.5, 0.5 - 0.8, 0.8 - 0.9, and >0.9, respectively. Furthermore, intra-observer, inter-observer, and inter-scan coefficients of variation (CV) were calculated for segmental mean T1. The CV was calculated as  $\text{CV} = 100\% * \text{SD}_{\text{paired difference}} / \text{Mean}$ . Scatter plots and Bland-Altman plots were created to visualize the agreement of T1 values.

### *Correlation with AAA diameter & ILT thickness*

Correlation with AAA diameter was tested for global mean T1, SD of global mean T1, global median T1, global min T1, and global max T1. Correlation with segmental ILT

thickness was tested for segmental mean T1, SD of segmental mean T1, segmental median T1, segmental min T1, segmental max T1, and the calculated madT1. Correlations were tested using Spearman's rho ( $\rho$ ) because of the small sample-size. Correlations were considered negligible, low, moderate or high when  $<0.30$ ,  $0.30 - 0.50$ ,  $0.50 - 0.70$  and  $>0.70$ , respectively.

### *Other analyses*

Inter-subject heterogeneity was tested with the Kruskal-Wallis test for the global median T1 values. Global median T1 values were also compared between inner and outer ILT layers with the Mann Whitney U test. Non-parametric tests with median values were chosen because of the small sample size. All statistical analyses were carried out with SPSS (version 25, IBM Corp, Armonk, NY, USA). A p value of  $< .05$  was considered significant.

## RESULTS

### Participants

At the time of writing, 19 patients were scanned for the 'Advanced MRI in AAA' study. Seven of them were excluded because of ILT absence. Another two participants were excluded because of motion artefacts in the scans. As a consequence, ten patients were included in the current analysis. Baseline patient characteristics are listed in Table 1. Eight of ten patients were male and median age was 71 years (Table 1). The median anteroposterior AAA diameter was 47 mm.

The aortic wall circumference was not entirely covered by ILT in all AAAs. As a consequence, not all AAAs had 6 ILT segments, resulting in a total of 50 instead of 60 ILT segments available for analysis.

### Outcome data

The T1 map of one subject is presented in Figure 1. Global mean T1 was  $1381.1 \pm 449.9$  ms and SD of global mean T1 was  $273.9 \pm 61.5$  ms. madT1 was  $-22.7 \pm 209.1$  ms. Mean T1 in the inner and outer ILT layer was  $1546.4 \pm 422.3$  ms and  $1286.5 \pm 497.2$  ms, respectively. The inner-to-outer ratio varied from 0.99 to 1.72 ms (Table 5), yet the difference between inner and outer (median) T1 values was not statistically significant ( $p = 0.22$ ). The mean T1 value of the blood in the aortic lumen was  $1688.0 \pm 163.7$  ms. Other T1 relaxation times are listed in Table 2. T1 relaxation times for individual subjects are listed in Table 5. Global mean T1 values ranged widely from 773.4 to 1992.1 between subjects. Yet, the global median T1 values were not significantly different between subjects ( $p = 0.44$ ). Mean global  $R^2$  was  $0.998 \pm 0.001$ , demonstrating a good fit of the model to the data.

**Table 1.** Baseline characteristics of 10 patients

Age, median (IQR) (y)	72 (65 - 77)
Age, mean $\pm$ SD (y)	71 $\pm$ 6
Male sex	8/10
Median max AAA diameter (mm)	47.5
Mean max AAA diameter (mm)	47.1
Median max ILT thickness (mm)	19.0
Mean max ILT thickness (mm)	15.9
Comorbidities	
- hypertension	5/10
- other cardiovascular disease	4/10
- COPD	2/10
- diabetes mellitus	2/10
Anticoagulants (total)	6/10
- platelet aggregation inhibitors	4
- unknown anticoagulants	2

**Table 2.** Results

	<b>n = 10</b>
global mean T1	1381.1 $\pm$ 449.9 1361.1 (957.3 - 1799.5)
SD of global mean T1	273.9 $\pm$ 61.5 256.3 (229.7 - 322.9)
global median T1	1358.1 $\pm$ 463.7 1312.0 (919.5 - 1847.3)
global minimum T1	730.3 $\pm$ 400.7 806.0 (351.8 - 1101.5)
global maximum T1	2106.1 $\pm$ 314.9 2132.0 (1808.5 - 2333.5)
madT1 *	-22.7 $\pm$ 209.1 10.7 (-146.6 - 107.5)
Aortic lumen mean T1	1688.0 $\pm$ 163.7 1699.3 (1563.1 - 1843.0)
R <sup>2</sup> value	0.998 $\pm$ 0.001 0.998 (0.997 - 1.000)
Inner layer mean T1	1546.4 $\pm$ 422.3 1602.6 (1149.8 - 1980.2)
Outer layer mean T1	1286.5 $\pm$ 497.2 1255.4 (794.6 - 1831.7)

Numbers are in milliseconds (ms) and are reported as mean  $\pm$  standard deviation and as median (interquartile range). \* Based on a total of 50 ILT segments.

**Table 3.** Intraclass correlation coefficients (ICC) for intra-observer, inter-observer and inter-scan agreement

	Intra-observer* ICC (95% CI)	Inter-observer† ICC (95% CI)	Inter-scan* ICC (95% CI)
Global mean T1 (n=10)	0.99 (0.95 - 1.00)	0.98 (0.80 - 1.00)	0.99 (0.98 - 1.00)
Global median T1 (n=10)	0.99 (0.97 - 1.00)	0.99 (0.93 - 1.00)	1.00 (0.99 - 1.00)
Segmental mean T1 (n=50)	0.98 (0.97 - 0.99)	0.96 (0.93 - 0.98)	0.96 (0.93 - 0.98)
Segmental median T1 (n=50)	0.91 (0.84 - 0.95)	0.91 (0.84 - 0.95)	0.87 (0.77 - 0.93)

\* Two-way mixed-effects model, † Two-way random-effects model

## Main results

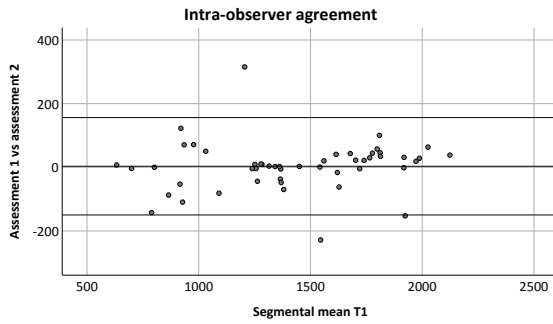
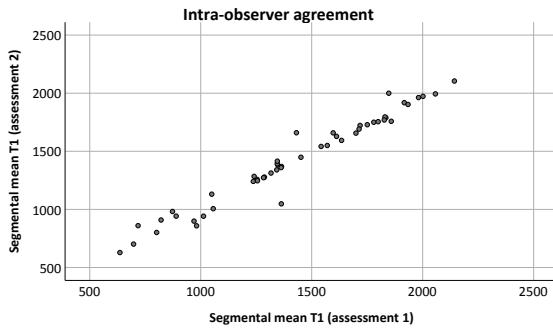
Excellent intra-observer, inter-observer and inter-scan agreement was found for mean and median T1 values of the 10 global ILTs (Table 3). With regard to the 50 ILT segments, excellent agreements were observed for all items except for the inter-scan agreement of the segmental median T1 which showed a good agreement (ICC 0.87 [95% CI 0.77 - 0.93], Table 3). Intra-observer, inter-observer and inter-scan CV of segmental mean T1 was 5.47%, 7.42%, and 7.67%, respectively. Figure 2 visualizes the intra-observer, inter-observer and inter-scan agreement in scatter plots and Bland Altman plots.

A statistically-significant low correlation was found between ILT thickness and SD of segmental mean T1 ( $\rho = 0.47$ ,  $p = 0.001$ ), Table 4, Figure 3). ILT thickness was not significantly correlated to the other T1 values, including madT1. Also, no correlation was found between AAA diameter and any of the global T1 values (Table 4, Figure 3).

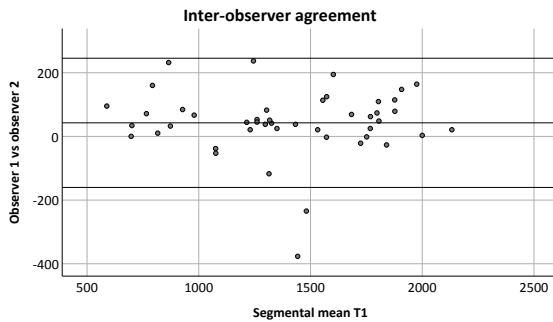
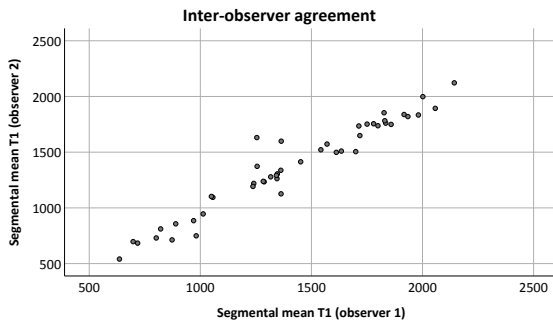
## DISCUSSION

This study shows that T1 mapping of intraluminal thrombus in AAAs is technically feasible. Out of twelve patients with ILT presence, ten were successfully included in the analysis. The excellent intra-observer, inter-observer, and inter-scan agreements demonstrate that the T1 mapping results are also reproducible. The results indicate that T1 mapping could be a valuable tool to quantitatively assess ILT composition. A significant correlation was observed between ILT thickness and the SD of segmental mean T1. This suggests that thicker ILT segments are more heterogeneous in composition. Furthermore, mean T1 values were higher in the inner ILT layers than in the outer layers in all but one AAA (mean 1546 and 1287 ms respectively). This could support the hypothesis of a layered structure within the ILT. The fact that the T1 values of the inner layers were closer to the T1 values of the flowing blood (1688 ms) also corresponds to previous studies reporting that canaliculi are mostly limited to the first 1 cm on the luminal side of the ILT.<sup>3</sup> The difference between inner and outer T1 values could also be a reflection of different ageing stages of the ILT.

A



B



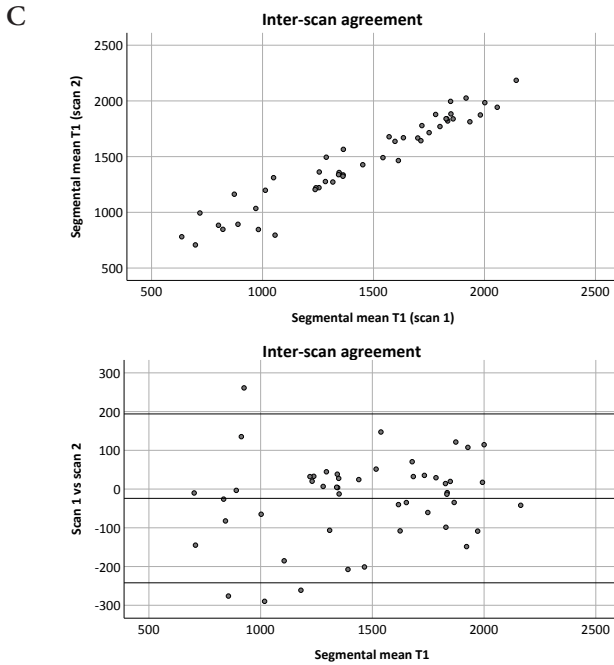


**Figure 2.** Scatter plots and Bland Altman plots for the intra-observer (a), inter-observer (b), and inter-scan (c) agreement for segmental mean T1.

Despite the excellent agreement results, the Bland Altman plots did reveal a small systematic error for the intra-observer and inter-scan agreement (Figure 2b and 2c). The Bland Altman plot of the inter-scan agreement (Figure 2c) also demonstrated a smaller amount of agreement for the lower T1 values. It is difficult to provide an explanation for this observation but it could be hypothesized that areas with lower T1 values (e.g. outer layers) were subject to more motion artefacts or variation in the manual segmentation.

Another interesting observation of this study was the high within-subject and inter-subject heterogeneity, as demonstrated by the high SD of global mean T1 within individual subjects (up to 402.7 ms, Table 5) and across all subjects (SD 449.9 ms, at a mean of 1381.1 ms, Table 2). The high inter-subject variability is also demonstrated by the wide range of global mean T1 between subjects (773.4 to 1992.1 ms, Table 5). Even though the inter-subject variability was not statistically significant, this does support the use of values such as madT1 that are not affected by inter-subject variability. The high inter-subject variability corresponds to similar studies that carried out T2 mapping of the myocardium.<sup>18</sup>

**Table 4.** Correlation between ILT thickness and segmental T1 values (a), and between AAA diameter and global T1 values (b) (Spearman's rho)

ILT thickness		
n = 50	Correlation coefficient	p-value
segmental mean T1	0.03	0.86
SD of segmental mean T1	0.47	0.001
segmental median T1	-0.03	0.86
segmental min T1	-0.27	0.06
segmental max T1	0.20	0.18
madT1	-0.01	0.97

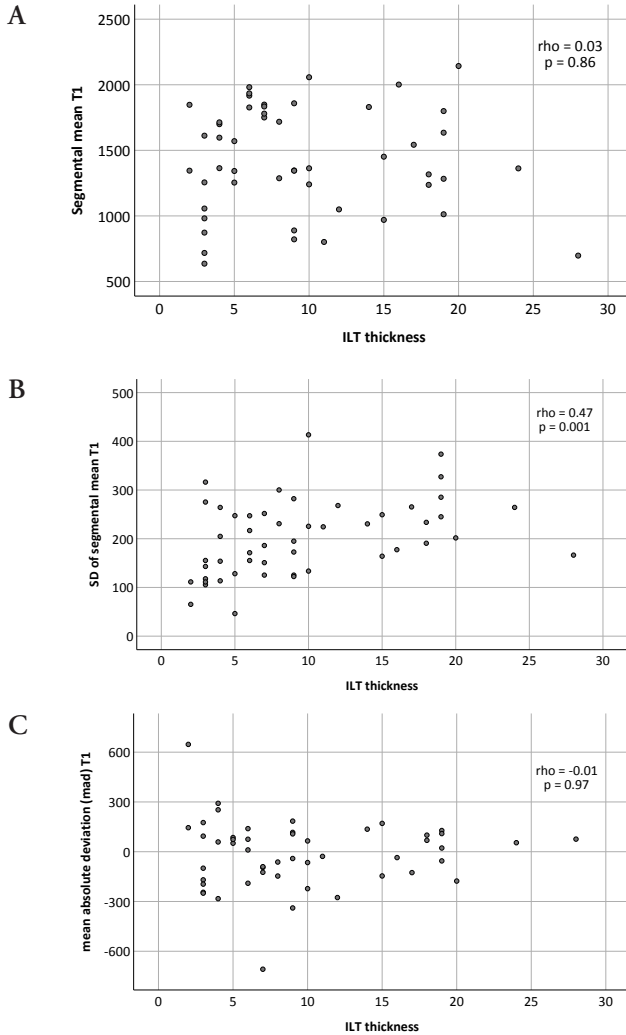
  

AAA diameter		
n = 10	Correlation coefficient	p-value
global mean T1	-0.02	0.96
SD of global mean T1	0.08	0.83
global median T1	-0.02	0.96
global min T1	-0.06	0.88
global max T1	-0.07	0.86

**Table 5.** Global T1 values per patient

Patient	AAA diameter	Mean T1	SD of mean T1	Median T1	Minimum T1	Maximum T1	Inner/outer ratio of mean T1
1	63	1140.5	402.72	1046	371	2198	1.45
2	46	1305.5	226.95	1301	770	1848	1.18
3	36	1655.7	251.48	1655	1062	2326	0.99
4	35	811.7	332.72	816	45	1690	1.72
5	34	1005.8	269.6	954	579	2066	1.30
6	45	1992.1	192.35	1968	1221	2356	1.07
7	49	1744.0	319.6	1814	842	2306	1.32
8	52	1416.6	258.64	1323	899	2065	1.28
9	50	1966.1	253.91	1947	1220	2598	1.10
10	61	773.4	230.65	757	294	1608	1.51

To our knowledge, no studies have investigated either T1 or T2 mapping of ILT. Therefore, the currently observed T1 values of ILT cannot be compared to previous studies. However, the measured T1 values of the blood in the aortic lumen ( $1688.0 \pm 163.7$ ms) were close to previous reports demonstrating native T1 values of  $1736 \pm 139$  ms in the blood at 3.0 T.<sup>19</sup>



**Figure 3.** Scatter plots demonstrating the relation between ILT thickness and segmental mean T1 (a), SD of segmental mean T1 (b), and madT1 (c).

### Strength and limitations

This report describes the preliminary results of the T1 mapping study and includes the first 10 scanned patients. The small sample size of 10 global ILTs was especially a limitation for the correlation analyses with AAA diameter. As a consequence, the results are difficult to extrapolate and possibly subject to type II errors. On the other hand, the correlation



analyses with ILT thickness included 50 ILT segments, which was large enough to detect one statistically significant association (i.e. between ILT thickness and SD of segmental mean T1). Because of the small sample size, non-parametric tests were used to analyze the data and the distribution of the data was not assessed. Another limitation of the current study was the exclusion of patients with very thin ILT. This was done because of the difficulty to create segmentations of the small areas, and the likelihood of including parts of the aortic lumen or aortic wall which would distort the results, especially when considering the movement of the patient and aorta during the breathhold. Further bias was minimized by using an identical scanning protocol for all patients.

### **Future perspectives**

At the time of writing, the inclusion of patients is ongoing in the 'Advanced MRI in AAA' study. If the final study with 20 patients confirms the presented results, the T1 mapping method will be worthwhile to investigate further in a prospective longitudinal study. Patient could be scanned repeatedly over the years to detect ILT growth patterns and to determine the T1 values of new and old areas of ILT. In addition to our current quantitative analysis, future studies could additionally assess qualitative patterns of T1 distribution within ILT. Moreover, post-contrast T1 maps could be used to search for possible fissures and permeability differences within ILT. To investigate the composition of ILT more precisely, pixel-by-pixel matrices of the T1 map could also be created to determine the correlation between T1 values and the distance from the central lumen line.

In order to increase our understanding of ILT and AAA development, future studies also need to address the interactions between ILT and adjacent structures. ILTs develop in a dynamic environment and are subject to effects from the aortic wall and the aortic lumen. The T1 mapping sequence could be used to compare ILT T1 values with results from other MR sequences. The T1 values of the ILT surface bordering the lumen could for example be compared to blood velocity and wall shear stress profiles as obtained with 4D flow sequences. The direct relation between certain areas of ILT growth and adjacent blood flow patterns can then be estimated.

It is not to be expected that T1 mapping will be used as a rupture prediction tool in the future. It could be considered as a valuable tool to monitor ILT and AAA progression which, in turn, could provide more information about the natural history of both ILT and AAA. The fact that the sequence can be carried out within seconds, and that post-processing can be performed within minutes, makes this tool easy to implement and easy to combine with other MR sequences.

## **ACKNOWLEDGMENTS**

We would like to thank the patients who participated in this study, and MRI technicians Sandra van den Berg - Faay and Raschel Snoeks for their assistance in the scanning process.

## REFERENCES

1. Kent KC. Clinical practice. Abdominal aortic aneurysms. *N Engl J Med*. 2014;371(22):2101-8.
2. Falk E. Dynamics in thrombus formation. *Ann N Y Acad Sci*. 1992;667:204-23.
3. Adolph R, Vorp DA, Steed DL, Webster MW, Kameneva MV, Watkins SC. Cellular content and permeability of intraluminal thrombus in abdominal aortic aneurysm. *J Vasc Surg*. 1997;25(5):916-26.
4. Fontaine V, Jacob MP, Houard X, Rossignol P, Plissonnier D, Angles-Cano E, et al. Involvement of the mural thrombus as a site of protease release and activation in human aortic aneurysms. *Am J Pathol*. 2002;161(5):1701-10.
5. Vorp DA, Lee PC, Wang DH, Makaroun MS, Nemoto EM, Ogawa S, et al. Association of intraluminal thrombus in abdominal aortic aneurysm with local hypoxia and wall weakening. *J Vasc Surg*. 2001;34(2):291-9.
6. Kazi M, Thyberg J, Religa P, Roy J, Eriksson P, Hedin U, et al. Influence of intraluminal thrombus on structural and cellular composition of abdominal aortic aneurysm wall. *J Vasc Surg*. 2003;38(6):1283-92.
7. Mower WR, Quinones WJ, Gambhir SS. Effect of intraluminal thrombus on abdominal aortic aneurysm wall stress. *J Vasc Surg*. 1997;26(4):602-8.
8. Wang DH, Makaroun MS, Webster MW, Vorp DA. Effect of intraluminal thrombus on wall stress in patient-specific models of abdominal aortic aneurysm. *J Vasc Surg*. 2002;36(3):598-604.
9. Haller SJ, Crawford JD, Courchaine KM, Bohannon CJ, Landry GJ, Moneta GL, et al. Intraluminal thrombus is associated with early rupture of abdominal aortic aneurysm. *J Vasc Surg*. 2018;67(4):1051-8 e1.
10. Puntmann VO, Peker E, Chandrashekar Y, Nagel E. T1 Mapping in Characterizing Myocardial Disease: A Comprehensive Review. *Circ Res*. 2016;119(2):277-99.
11. Coolen BF, Poot DH, Liem MI, Smits LP, Gao S, Kotek G, et al. Three-dimensional quantitative T1 and T2 mapping of the carotid artery: Sequence design and in vivo feasibility. *Magn Reson Med*. 2016;75(3):1008-17.
12. Messroghli DR, Moon JC, Ferreira VM, Grosse-Wortmann L, He T, Kellman P, et al. Clinical recommendations for cardiovascular magnetic resonance mapping of T1, T2, T2\* and extracellular volume: A consensus statement by the Society for Cardiovascular Magnetic Resonance (SCMR) endorsed by the European Association for Cardiovascular Imaging (EACVI). *J Cardiovasc Magn Reson*. 2017;19(1):75.
13. World Medical A. World Medical Association Declaration of Helsinki: ethical principles for medical research involving human subjects. *JAMA*. 2013;310(20):2191-4.
14. von Elm E, Altman DG, Egger M, Pocock SJ, Gøtzsche PC, Vandenbroucke JP, et al. The Strengthening of Reporting of Observational Studies in Epidemiology (STROBE) statement: guidelines for reporting observational studies. *J Clin Epidemiol*. 2008;61(4):344-9.
15. Baessler B, Schaarschmidt F, Dick A, Stehning C, Schnackenburg B, Michels G, et al. Mapping tissue inhomogeneity in acute myocarditis: a novel analytical approach to quantitative myocardial edema imaging by T2-mapping. *J Cardiovasc Magn Reson*. 2015;17:115.
16. Baessler B, Schaarschmidt F, Treutlein M, Stehning C, Schnackenburg B, Michels G, et al. Re-evaluation of a novel approach for quantitative myocardial oedema detection by analysing tissue inhomogeneity in acute myocarditis using T2-mapping. *Eur Radiol*. 2017;27(12):5169-78.

17. Koo TK, Li MY. A Guideline of Selecting and Reporting Intraclass Correlation Coefficients for Reliability Research. *J Chiropr Med.* 2016;15(2):155-63.
18. Baessler B, Schaarschmidt F, Stehning C, Schnackenburg B, Maintz D, Bunck AC. A systematic evaluation of three different cardiac T2-mapping sequences at 1.5 and 3T in healthy volunteers. *Eur J Radiol.* 2015;84(11):2161-70.
19. Dabir D, Child N, Kalra A, Rogers T, Gebker R, Jabbour A, et al. Reference values for healthy human myocardium using a T1 mapping methodology: results from the International T1 Multicenter cardiovascular magnetic resonance study. *J Cardiovasc Magn Reson.* 2014;16:69.